ELSEVIER

Journal of Power Sources 113 (2003) 109–114

JOURNAL OF POWER SOURCES

www.elsevier.com/locate/jpowsour

Three-dimensional thermo-fluid electrochemical modeling of planar SOFC stacks

K.P. Recknagle*, R.E. Williford, L.A. Chick, D.R. Rector, M.A. Khaleel

Pacific Northwest National Laboratory, P.O. Box 999 MSIN K7-15, Richland, WA 99352, USA

Received 30 August 2002; accepted 12 September 2002

Abstract

A simulation tool for modeling planar solid oxide fuel cells is demonstrated. The tool combines the versatility of a commercial computational fluid dynamics simulation code with a validated electrochemistry calculation method. Its function is to predict the flow and distribution of anode and cathode gases, temperature and current distributions, and fuel utilization. A three-dimensional model geometry, including internal manifolds, was created to simulate a generic, cross-flow stack design. Similar three-dimensional geometries were created for simulation of co-flow, and counterflow stack designs. Cyclic boundary conditions were imposed at the top and bottom of the model domains, while the lateral walls were assumed adiabatic. The three cases show that, for a given average cell temperature, similar fuel utilizations can result irrespective of the flow configuration. Temperature distributions however, which largely determine thermal stresses during operation, are dependent on the chosen design geometry/flow configuration. The co-flow case had the most uniform temperature distribution and the smallest thermal gradients, thus offers thermo-structural advantages over the other flow cases.

Keywords: Solid oxide fuel cell; Three-dimensional model; Fuel utilization; Current and temperature distribution

1. Introduction

The planar-type solid oxide fuel cell (SOFC) is desirable for many applications due to its compactness. Cell active areas can be stacked in close proximity to yield large power densities. Development of the planar SOFC has challenges related to the high-temperature operation (600–1000 °C). Many designs use excess cathode airflow to remove heat during steady-state operation. The distribution and utilization of fuel over the anode and the distribution of relatively cooler cathode air interact to determine the temperature gradients. One of the many challenges associated with developing this type of SOFC is to minimize the non-uniform temperature distributions that contribute to stress in the planar components (stress analyses are not reported in this paper).

Fuel utilization and average cell temperature are controlled by the delivery rate and the temperatures of fuel and air to the cell. Fuel distribution is critical due to the exothermic electrochemical reactions: cell areas covered by concentrated fuel become electrochemically active, leading to increased local temperatures, which yields even faster reaction rates. Cell areas covered by depleted fuel become inactive, thus cooler, which leads to even slower localized reaction rates. Increased fuel flow tends to increase uniformity of the reaction rates across the active area and to decrease fuel utilization. Decreased fuel flow tends to increase fuel utilization, but can cause local fuel depletion and cold spots that exacerbate temperature non-uniformities. Air and fuel inlet temperatures also affect the reaction rates, cell temperature, and the fuel utilization. Therefore, management of the flow of air and fuel, and the distribution of each, is critical to stable operation of the cell. Other factors that affect the temperature distribution and fuel utilization are the relative orientations of the fuel and airflows, the mass and dimensions of the cell components, and dimensions of flow channels. Thus, geometry is important in establishing a well-operating cell. In order to efficiently develop and optimize planar SOFC stacks, it is convenient to have the capability to experiment numerically with the effects of geometric configurations on operation and performance.

Modeling of the planar SOFC during steady operation to calculate temperatures and stresses is ongoing and becoming increasingly three-dimensional [1–3]. Investigations of planar SOFC operation [4] and planar SOFC performance [5] have predicted cell temperature and electrical current distributions for various flow configurations. The purpose of the

* Corresponding author. Tel.: +1-509-372-4840; fax: +1-509-375-3865.
E-mail address: kp.recknagle@pnl.gov (K.P. Recknagle).

0378-7753/02/$ – see front matter
PII: S0378-7753(02)00487-1

Nomenclature

$F_{h,j}$	diffusional energy flux in direction x_j
$\sqrt{g}$	determinant of metric tensor
h	enthalpy
I_{ave}	average electrical current, A/cm^2
m_m	mass fraction of mixture component m
M_m	molecular weight of mixture component m
p	piezometric pressure
R	universal gas constant
s_h	enthalpy source term
s_i	momentum source components
s_m	mass source term
T	absolute temperature, Kelvin
T_{PEN}	average cell (or PEN) temperature
ΔT_{PEN}	difference between maximum and minimum temperature on active area of cell
u_i	fluid velocity component in direction x_i
$\tilde{u}_j$	fluid velocity relative to coordinate system moving with velocity u_{cj}
V	voltage
x_i	Cartesian coordinate ($i = 1, 2, 3$)

Greek Letters

ρ	density, kg/m^3
τ_{ij}	stress tensor component

present work is to demonstrate a modeling tool to predict the fuel utilization, electric current, and temperature distributions in planar SOFC stacks with arbitrary three-dimensional geometries. For this study, cross-, co-, and counterflow configurations are examined.

The modeling tool couples a validated electrochemistry calculation method with a commercial computational fluid dynamics (CFD) simulation code. In the calculations, the code solves the finite-volume Navier–Stokes and transport equations to obtain the flow, species concentrations, and temperature at each location in the cell/stack. This information is passed to the electrochemistry module (subroutine). Here the local current density is calculated, based on the temperature, applied cell voltage, and pressures. The current is then used to calculate the hydrogen combustion rate. The water-gas shift reaction rate is assumed to maintain equilibrium conditions. Heat generation rates and species source (fuel/air) rates are supplied to the code based on the hydrogen combustion and shift reaction rates. Gas species concentrations and temperature distributions are then calculated for the next iteration, and so on, until equilibrium is achieved for the shift reaction.

2. Modeling approach

The repeating unit of a typical planar SOFC stack is constructed of a positive electrode–electrolyte–negative electrode (PEN) and an interconnect plate "stacked" together. Fig. 1 shows a schematic of an interconnect plate. The schematic is displayed as being transparent to show top and bottom features. In this example, the interconnect is formed to create internal gas flow manifolds and flow passages above and below the plate in a cross-flow configuration. The active cell area in Fig. 1 is that formed by the intersection of air and fuel flows in the X–Y plane. A cell unit (or single-cell stack) is formed when interconnects, similar to that in Fig. 1, are placed above and below a PEN. Fig. 2 shows a partial schematic view of a vertical slice through a Y–Z plane of a multiple-cell, cross-flow stack. As in Fig. 1, air flows along the Y-direction. Fuel flow is along the X-direction. Fuel flow vectors are orthogonal to the page and are represented in Fig. 2 by X in the fuel region. The location of a cell unit along Z is shown at left in the figure.

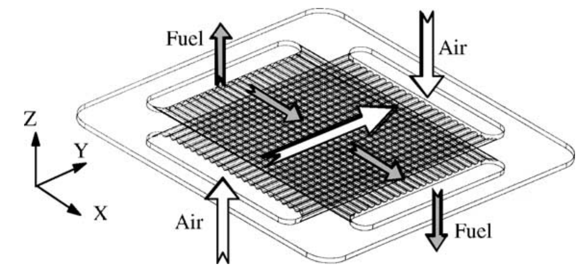

Fig. 1. Schematic view of a typical cross-flow planar interconnect plate.

A generic single-cell, cross-flow, stack model, including internal manifolds, was created for benchmark calculations of the fuel utilization, gas, temperature, and electrical current distributions. The model represented a repeating cell unit residing in the center of a large stack such that no end effects were present at the cell of interest. The mesh contained 23 elements along the X- and Y-directions (529 elements) to resolve a rectangular 116.6 cm^2 active cell area on the PEN. The 760 mm thick PEN was modeled as a monolithic structure containing one element in the Z-direction. Fuel and air passages above and below the PEN each were subdivided into three elements. Individual flow channels created by webs in the interconnect (as in Fig. 1) were

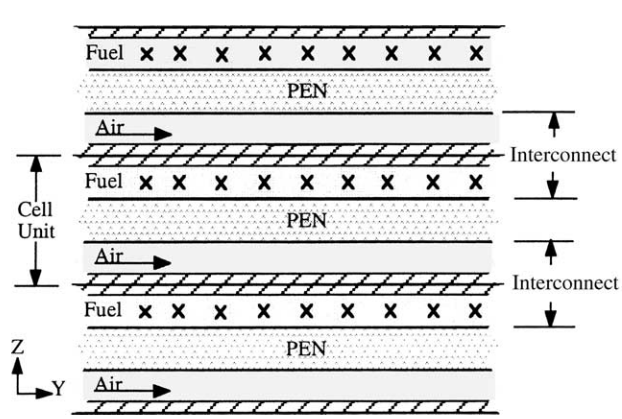

Fig. 2. Schematic section view of a typical cross-flow stack. X in the fuel region represent fuel flow vectors perpendicular to the page.

not modeled. Instead, we assumed that the region was one large flow passage and a material placed in the region would act as current collector and make the electrical contact between PEN and interconnect. A glass seal between the PEN and interconnect was included in the model. The three-dimensional model containing one repeating cell unit (with PEN, air and fuel channels, glass seal, and 1/2 interconnect thickness top and bottom, in the Z-direction) including internal gas flow manifolds contained 26,255 computational elements. Mesh resolution was chosen based on simulation run-time/accuracy tests and represents an optimized mesh.

2.1. Thermo-fluid model

The widely used STAR-CD [6] code was selected for the thermo-fluids calculations and as host for the electrochemistry calculations. The electrochemistry calculations will be discussed in a later section. STAR-CD is a CFD code that solves the algebraic finite-volume equations. For each of the computational mesh elements, in the fluid regions, STAR-CD solved the Navier–Stokes equations for conservation of mass

$$\frac{1}{\sqrt{g}}\frac{\partial}{\partial t}(\sqrt{g}\rho) + \frac{\partial}{\partial x_j}(\rho \tilde{u}_j) = s_m \qquad (1)$$

and momentum

$$\frac{1}{\sqrt{g}}\frac{\partial}{\partial t}(\sqrt{g}\rho u_i) + \frac{\partial}{\partial x_j}(\rho \tilde{u}_j u_i - \tau_{ij}) = -\frac{\partial p}{\partial x_i} + s_i \qquad (2)$$

as well as the conservation of enthalpy:

$$\frac{1}{\sqrt{g}}\frac{\partial}{\partial t}(\sqrt{g}\rho h) + \frac{\partial}{\partial x_j}(\rho \tilde{u}_j h - F_{h,j}) = \frac{1}{\sqrt{g}}\frac{\partial}{\partial t}(\sqrt{g}p) + \frac{\partial}{\partial x_j}(\tilde{u}_j p) - p\frac{\partial u_j}{\partial x_j} + \tau_{ij}\frac{\partial u_i}{\partial x_j} + s_h \qquad (3)$$

In the solid regions, STAR-CD conserved specific energy. The equation is similar to (3) without the pressure terms. Both the air and fuel streams were modeled as ideal gas mixtures with density given by:

$$\rho = \frac{p}{RT}\left(\sum_m \frac{m_m}{M_m}\right) \qquad (4)$$

where m_m is the mass fraction of a component with molecular weight M_m. Specific heats of the gaseous mixtures were calculated as mass weighted averages of the component values. Gas viscosities and thermal conductivities were taken to be constant at the average cell temperature.

Heat transfer between the fluid and solid materials was limited to conduction and convection. The flow channels had large aspect ratios (length-to-height, roughly 100:1 on the cathode side and 200:1 on the anode side) such that view factors for radiant heat exchange downstream were small. Additionally, the geometric form of the material used for current collection would obstruct and further reduce the contribution of thermal radiation in the downstream direction. The effect of radiation, therefore, was small relative to the other modes of heat transfer and was neglected in the calculations.

Table 1
Solid material properties

Cell Component	Density (kg/m^3)	Thermal conductivity (W/m K)	Specific heat (J/kg K)
Interconnect	7700	13	0.8
PEN	4200	2	0.623
Glass Seal	2500	1.4	0.6

Solid material properties used in the calculations are listed in Table 1. Specific heats were reduced by factor 10^3 to expedite the calculations. This is an acceptable practice for steady-state simulations.

2.2. Boundary conditions

The single-cell stack model represented a repeating cell unit in the center of a large stack; cyclic boundary conditions were imposed at the top and bottom of the model domain (i.e. Z-direction in Figs. 1 and 2). Walls at the periphery of the stack (at the X- and Y-direction extremes) were assumed adiabatic. Constant temperature, velocity, and gaseous composition were imposed at the inflow boundaries for the fuel and air.

2.3. Electrochemical model

The unit cell electrochemistry model (UCEM) predicts local electrical responses to changes in fuel flow rate, local fuel composition, and local temperature. The response characteristics are adjustable to component materials and dimensions as well as to electrode porosity. The model accounts for overpotentials due to Ohmic resistance of the cell components, contact resistance at electrode–current collector interfaces, charge transfer at the electrodes, and diffusion of reactants into and products out of the porous electrodes. The UCEM predicts the current–voltage (I–V) response curve based on the local conditions for a specific unit area within the active area of the cell. The model contains adjustable parameters, which are set by calibrating the model to I–V data obtained from operation of a small (1 in. diameter) single-cell SOFC under a range of fuel compositions and temperatures. Construction and calibration of the UCEM is described elsewhere [7,8].

2.4. Electrochemistry equations in STAR-CD

The interface between STAR-CD and the electrochemical (EC) model was implemented via the POSDAT routine in STAR-CD. POSDAT was called after each STAR-CD iteration. The EC model was called from within POSDAT for each PEN element in the model domain. Information passed included temperature, gas concentrations (in the adjacent fluid streams), and PEN voltage. Voltage, rather than current, is held constant across a PEN to facilitate multiple-cell stack simulations. A non-linear root solver was used to find the local electrical current on the PEN corresponding to the PEN voltage. The local current was found according to the UCEM. The Nernst voltage and overvoltages due to Butler–Volmer, resistive, and concentration polarizations are also calculated. A thermodynamic equilibrium constant for the water-gas shift reaction is then calculated for each PEN element using Gibb's free energies and the local temperature. This is compared to the local chemical equilibrium constant based on the instantaneous concentrations of each gas species in the reactions. Agreement between the two equilibrium constants, to within a small error, denotes convergence of the STAR-CD/EC simulation. Local PEN heat generation is also calculated during each iteration and provided to STAR-CD for the next iteration.

2.5. Calculations and results

Conditions for the benchmark cross-flow case were chosen to achieve average cell temperature and fuel utilization of roughly 750 °C and 60–70%, respectively, for a cell voltage of 0.7 V. Air was delivered to the cathode at 0.25 gm/s and 625 °C. The benchmark fuel was a PO_x-reformed gasoline with 45% anode recycle, delivered to the anode at 0.018 gm/s (9.5E − 4 mol/s) and 625 °C. Molar composition of the fuel was 36% H_2, 35% CO, 5% H_2O, 5% CO_2, and 19% N_2.

The resulting steady-state cell (PEN) average temperature was 769 °C with maximum and minimum PEN temperatures of 643 and 912 °C, respectively. Fuel utilization was 61.7%. The PEN temperature distribution for this case is presented in Fig. 3. The temperature was highest near the fuel inlet and air outlet. The Nernst potential and reaction rates on the PEN

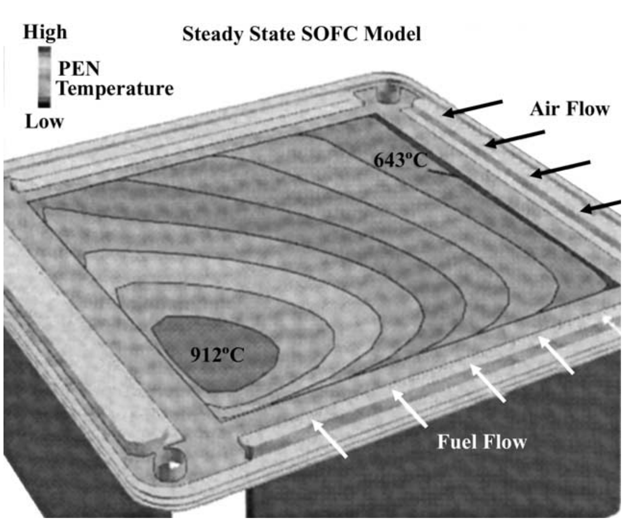

Fig. 3. Predicted PEN temperature distribution for single-cell stack in cross-flow configuration. Temperature range: 643–912 °C (769 °C average).

Table 2
Operating conditions for single-cell stack simulations (cell voltage = 0.7 V)

Flow configuration	Air delivery		Fuel delivery	
	gm/s	°C	gm/s	°C
Cross-flow	0.25	625	0.018	625
Co-flow	0.25	625	0.018	625
Counterflow	0.25	595	0.018	595

were highest near the fuel inlet and decreased in the direction of the fuel flow. Air flowing past the PEN was most effective at cooling near the air inlet and carried heat generated in the PEN toward the air outlet, thus moving the "hot spot" toward the air outlet.

An attempt to achieve a more uniform temperature distribution led to an investigation into the effect of cell geometry on the fuel/air distributions and fuel utilization. In addition to the cross-flow case, cases with co-flow and counterflow configurations were generated. Active area, flow passage heights, and interconnect dimensions from the cross-flow case were all retained. Operating conditions for these other cases were adjusted to roughly reproduce the fuel utilization and average cell temperature obtained by the cross-flow case. Conditions (delivery rates and temperatures of the air and fuel streams) are listed in Table 2.

Results from the three flow configuration cases are shown in Figs. 4–6, and listed in Table 3. Temperatures are shown in Fig. 4. Current density distributions are shown in Fig. 5. Mass concentration of the hydrogen is shown in Fig. 6. Cell temperature difference, average cell temperature, current density, and fuel utilization are itemized in Table 3.

The cross-flow PEN temperature distribution on the active cell area is shown in plan view in Fig. 4a. Also in Fig. 4 are the cell area temperatures for the co-flow (Fig. 4b) and counterflow (Fig. 4c) cases. In each case the temperature increased along the airflow direction (top to bottom in Figs. 4a–c), reaching a maximum near the air exit. Of the three flow configurations tested, the co-flow case had the most uniform temperature distribution and smallest temperature difference (ΔT) from air inlet to outlet. This is due to offsetting effects of air near the inlet, at its coolest, being aligned with the fuel inlet where the Nernst potential is highest. Cross- and counterflow cases had ΔTs of similar magnitude across the PEN (see Table 3), both larger than that of the co-flow case by more than 80 °C.

Table 3
Single-cell stack simulation results (cell voltage = 0.7 V)

Flow configuration	ΔT_{PEN} (°C)	T_{PEN} (°C)	I_{ave} (A/cm^2)	Fuel utilization (%)
Cross-flow	269	769	0.69	62
Co-flow	184	763	0.71	64
Counterflow	267	758	0.73	63

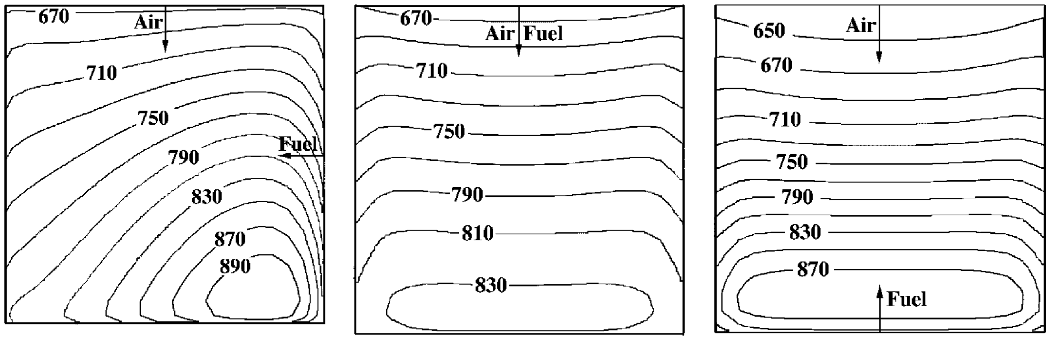

(a) Cross-Flow (b) Co-Flow (c) Counterflow

Fig. 4. Temperature distribution on the active cell area, °C.

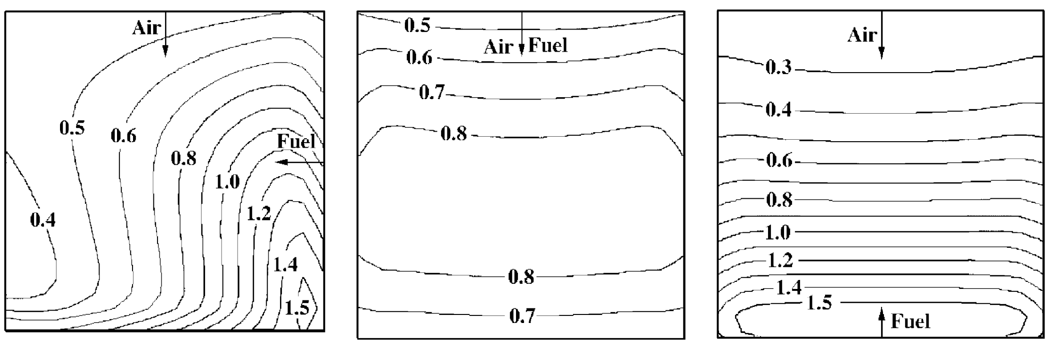

(a) Cross-Flow (b) Co-Flow (c) Counterflow

Fig. 5. Current density distribution on the active cell area, A/cm^2.

Consistent with the temperature distribution, the current density (see Fig. 5) was most uniform in the co-flow case. In the cross-flow and counterflow cases, current density was high near the fuel inlet and air outlet corresponding to high temperature and Nernst potential in that region. This result was not present in the co-flow case where the maximum current density was roughly midstream from inlet to exit—again due to the coincident location of air and fuel inlets that is a characteristic of the co-flow configuration.

Mass concentration of H_2 is shown for the three cases in Fig. 6. The primary difference was the two-dimensional nature of the cross-flow case. The co-flow and counterflow cases had low fuel concentration across the full width of the fuel outlet creating a ''line'' minimum. The cross-flow case had a ''point'' minimum that was lower in concentration than either of the other two cases. When trying to maximize fuel utilization, a ''line'' minimum (rather than a ''point'' minimum) would be more suitable to decrease the risk of localized fuel depletion. Preventing fuel depletion, and subsequent cold spots, contributes to smaller thermal gradients and less severe thermal stresses thus helping to ensure the structural integrity of the cell components.

Table 3 lists the cell (or PEN) ΔT, the average PEN temperature, current density, and fuel utilization for the three flow configuration cases. Of interest is the roughly 30% reduction of the ΔT in the co-flow case compared to the

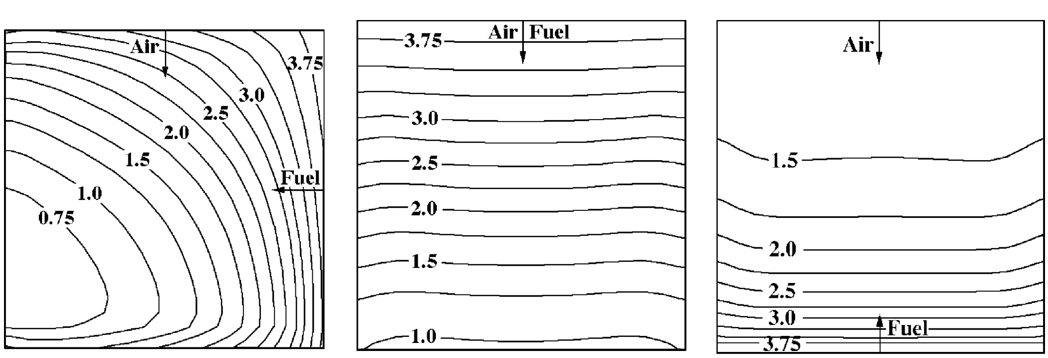

(a) Cross-Flow (b) Co-Flow (c) Counterflow

Fig. 6. Hydrogen distribution in the fuel stream adjacent to the active cell area. Mass percent H_2, $kg/kg \times 100\%$.

other flow cases. This occurs while average PEN temperature, current density, and fuel utilization differ by no more than 3% between the co-flow and either of the other two cases. The co-flow case, due to its relatively uniform temperature distribution and smaller thermal gradients, offers thermo-structural advantages over the other flow cases.

3. Summary and conclusions

A simulation tool for three-dimensional modeling of planar solid oxide fuel cells has been demonstrated. The tool combines a commercial CFD simulation code and a validated electrochemistry calculation method, enabling the calculations to be performed on complex, three-dimensional meshes. The effects of cell flow configuration on the distribution of temperature, current density, and fuel species was investigated. Three flow configurations, cross-flow, co-flow, and counterflow were examined using identical inflow rates and variable inflow temperatures. It was found that, for similar fuel utilization and average cell temperature, the co-flow case had the most uniform temperature distribution and the smallest thermal gradients, which is advantageous with respect to ensuring structural integrity of the stack components.

Acknowledgements

The work summarized in this paper was funded as part of the Solid-State Energy Conversion Alliance (SECA) Core Technology Program by the US Department of Energy's National Energy Technology Laboratory (NETL). PNNL is operated by Battelle Memorial Institute for the US Department of Energy under Contract DE-AC06-76RLO 1830.

References

[1] H. Yakabe, M. Hishunuma, M. Uratani, Y. Matsuzaki, I. Yasuda, Evaluation and modeling of performance of anode-supported solid oxide fuel cell, J. Power Sources 86 (2000) 423–431.
[2] H. Yakabe, T. Ogiwara, I. Yasuda, M. Hishunuma, Model calculation for planar SOFC focusing on internal stresses: solid oxide fuel cells (SOFC VI), in: Proceedings of the Sixth International Symposium, vol. 99 (19), 1999, pp. 1087–1098.
[3] H. Yakabe, T. Ogiwara, M. Hishunuma, I. Yasuda, 3-D model calculation for planar SOFC, J. Power Sources 102 (2001) 144–154.
[4] S.G. Neophytides, The reversed flow operation of a cross-flow solid oxide fuel cell monolith, Chem. Eng. Sci. 54 (1999) 4603–4613.
[5] M. Iwata, T. Hikosaka, M. Morita, T. Iwanari, K. Ito, K. Onda, Y. Esaki, Y. Sakaki, S. Nagata, Performance analysis of planar-type unit SOFC considering current and temperature distributions, Solid State Ionics 132 (2000) 297–308.
[6] STAR-CD Version 3.05 Methodology, Computational Dynamics Ltd, 1998.
[7] K. Keegan, M. Khaleel, L. Chick, K. Recknagle, S. Simner, J. Deibler, Analysis of a planar solid oxide fuel cell based automotive auxiliary power unit, in: Congress 2002 Proceedings, Society of Automotive Engineers, 2002-01-0413.
[8] L.A. Chick, J.W. Stevenson, K.D. Meinhardt, S.P. Simner, J.E. Jaffe, R.E. Williford, Modeling and performance of anode-supported SOFC, in: 2000 Fuel Cell Seminar—Abstracts, 2000, pp. 619–622.